Dalton Transactions

PAPER

View Article Online
View Journal

Cite this: DOI: 10.1039/c6dt03027k

Competing reaction pathways of 3,3,3-trifluoropropene at rhodium hydrido, silyl and germyl complexes: C–F bond activation *versus* hydrogermylation†

Theresia Ahrens, Michael Teltewskoi, Mike Ahrens, Thomas Braun* and Reik Laubenstein

Received 30th July 2016,
Accepted 6th October 2016

DOI: 10.1039/c6dt03027k

www.rsc.org/dalton

The reaction of the silyl complex [Rh{Si(OEt)$_3$}(PEt$_3$)$_3$] (**1**) with 3,3,3-trifluoropropene afforded the rhodium complex [Rh(CH$_2$CHCF$_3$){Si(OEt)$_3$}(PEt$_3$)$_2$] (**2**) which features a bonded fluorinated olefin. In contrast the rhodium hydrido complex [Rh(H)(PEt$_3$)$_3$] (**3**) yielded on treatment with 3,3,3-trifluoropropene in the presence of a base the fluorido complex [Rh(F)(PEt$_3$)$_3$] (**4**) together with 1,1-difluoro-1-propene by C–F bond activation. At low temperature the intermediate *fac*-[Rh(H)(CH$_2$CHCF$_3$)(PEt$_3$)$_3$] (**5**) was detected by NMR spectroscopy. The germyl complex [Rh(GePh$_3$)(PEt$_3$)$_3$] (**6**) reacted also with 3,3,3-trifluoropropene by C–F bond activation affording again the fluorido complex [Rh(F)(PEt$_3$)$_3$] (**4**) as well as the (3,3-difluoroallyl)-triphenylgermane **7**. The catalytic hydrogermylation of 3,3,3-trifluoropropene in the presence of various germanium hydrides under mild conditions was developed by employing complex **6** as a catalyst. The molecular structures of both germane derivatives (3,3-difluoroallyl)triphenylgermane **7** and 1,1,1-trifluoropropane-3-triphenylgermane **8** were determined by X-ray crystallography.

Introduction

Fluoroorganic compounds receive a lot of attention due to their broad field of applications as potential building blocks in pharmaceuticals, agrochemicals or in material science.[1–6] Therefore, it is not surprising that there is a continuing demand for the development of new routes to access fluorinated entities. The selective transition-metal mediated C–F bond activation represents a unique way to generate novel structural motifs.[7–34] Whereas a lot of stoichiometric or catalytic C–F bond derivatization reactions of fluorinated aromatics were reported,[35–46] examples for fluorinated alkenes are comparatively limited.[47–79] In most of the cases the conversions include C–C coupling[48–56,58–60] or hydrodefluorination[47,60–75] reactions.[31,32,80] The replacement of fluorine in poly- or perfluorinated molecules by a new functional group in order to obtain a higher valuable fluorinated building block still remains rare and challenging.[18,27,80–82] In previous work we demonstrated that the rhodium complexes [Rh(H)(PEt$_3$)$_3$] (**3**) or [Rh{(*Z*)-CF=CF(CF$_3$)}(PEt$_3$)$_3$] are suitable for a catalytic C–F bond transformation of hexafluoropropene in the presence of HBpin (pin = pinacolato) or tertiary silanes to afford fluoroalkyldioxaborolanes or 3,3,3-trifluoropropylsilanes, respectively.[78,79] Note that not in any of these cases a C–F activation and functionalization of the trifluoromethyl group was observed. However, Rieger *et al.* recently reported the catalytic activation of 3,3,3-trifluoropropene by cationic group IV metallocenes in the presence of an excess of triisobutylaluminum yielding in benzene 3,3-(difluoroallyl)-benzene and 1,1-difluoro-5-methyl-hex-1-ene.[83] Herein, we report on the reactivity of 3,3,3-trifloropropene with [Rh{Si(OEt)$_3$}(PEt$_3$)$_3$] (**1**), [Rh(H)(PEt$_3$)$_3$] (**3**) and [Rh(GePh$_3$)(PEt$_3$)$_3$] (**6**). The observed reaction routes involve coordination at the metal centre, hydrodefluorination, C–F bond activation and concomitant germylation, or catalytic hydrogermylation reactions.

Results and discussion

Treatment of the rhodium(I) silyl complex [Rh{Si(OEt)$_3$}(PEt$_3$)$_3$] (**1**) with 3,3,3-trifluoropropene afforded the alkene complex [Rh(CH$_2$CHCF$_3$){Si(OEt)$_3$}(PEt$_3$)$_2$] (**2**) by coordination of the fluorinated olefin and replacement of one phosphine ligand (Scheme 1). Complex **2** was only characterized in solution, because it is only stable in solution for about 1.5 hours. After this time the NMR spectroscopic data of the reaction solution

Humboldt-Universität zu Berlin, Department of Chemistry, Brook-Taylor-Straße 2, D-12489 Berlin, Germany. E-mail: thomas.braun@chemie.hu-berlin.de

†Electronic supplementary information (ESI) available. CCDC 1496565 and 1496566. For ESI and crystallographic data in CIF or other electronic format see DOI: 10.1039/c6dt03027k

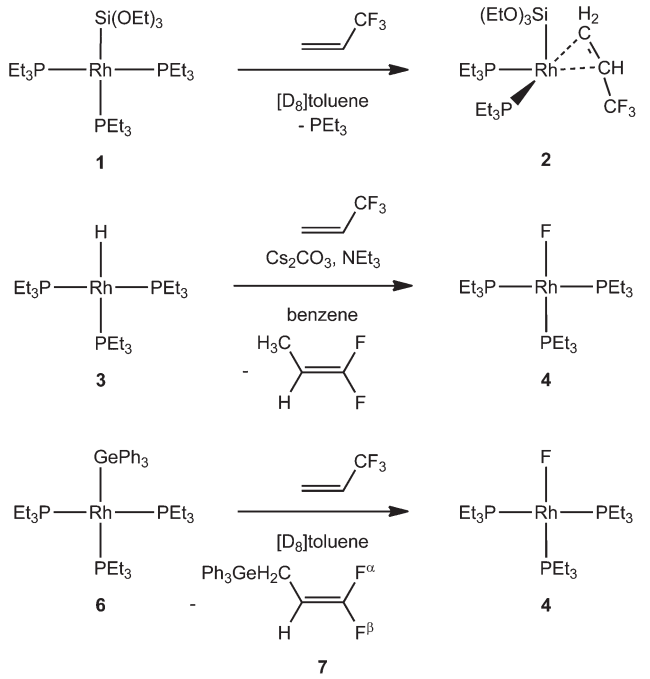

Scheme 1 Reaction of 3,3,3-trifluoropropene with rhodium(I) complexes.

reveal the formation of the starting compound **1** in addition to several unidentified rhodium species.[62,64,84] However, when the solvent, the excess of 3,3,3-trifluoropropene as well as the phosphine were removed under vacuum immediately after treatment of **1** with the fluorinated olefin, the formation of the rhodium fluorido complex $[Rh(F)(PEt_3)_3]$ (**4**) (ratio **2** : **4** = 4 : 1) was observed. The $^{31}P\{^1H\}$ NMR spectrum of **2** depicts a doublet of doublet of quartets at δ = 20.5 ppm ($^1J_{Rh,P}$ = 135, $^2J_{P,P}$ = 29 and $^4J_{P,F}$ = 19 Hz) and a doublet of doublets at δ = 19.3 ppm ($^1J_{Rh,P}$ = 137, $^2J_{P,P}$ = 29 Hz) with an integral ratio of 1 : 1 for the two inequivalent phosphine ligands. The former signal can presumably be assigned to the phosphorus atom in the *trans*-position to the $CHCF_3$ group, which also indicates a restricted rotation of the fluorinated olefin at the metal centre on the NMR time-scale. The ^{19}F NMR spectrum exhibits a multiplet signal at δ = −53.4 ppm which can be assigned to the CF_3 group. In a ^1H decoupling experiment it simplifies to a doublet with a fluorine phosphorus coupling constant of $^4J_{P,F}$ = 19 Hz. The ^1H, ^{29}Si HMBC NMR spectrum shows a cross peak at δ = −49 ppm in the ^{29}Si domain which correlates to the CH_2 and CH_3 groups of the ethoxy moieties as well as to the rhodium bonded CH_2 group of the η^2-coordinated trifluoropropenyl ligand. The chemical shift differs when compared to structurally related rhodium silyl complexes bearing no fluorinated ligand such as $[Rh\{Si(OR)_3\}(PEt_3)_3]$ [R = Et (δ = −11 ppm); Me (δ = −8 ppm)] or $[Rh\{Si(OEt)_3\}(CO)(PEt_3)_2]$ (δ = −10 ppm).[85,86] DFT calculations were run on conceivable rotational isomers of **2**. The structures exhibit a distorted square pyramidal coordination of the ligands at the metal center with the silyl ligand at the apical position and the CF_3 group either orientated towards the silyl ligand or the vacant coordination site (see also ESI†).

The calculations did not converge in any conceivable trigonal bipyramidal arrangements of the ligands. The isomer with the lowest energy (**2a**) in the gas phase exhibits an *anti* conformation of the silyl and CF_3 group as depicted in Fig. 1. The Rh–C [2.132 and 2.113 Å] and the C–C(CF_3) [1.442 Å] bond distances of **2a** indicate a considerable contribution of a mesomeric metallacyclopropane structure, although the $^1J_{Rh,P}$ coupling constants are in the typical range for rhodium(I) complexes (see below).[62,85,87,88] The C–C(CF_3) bond distance in the DFT-optimized structure of 3,3,3-trifluoropropene is 1.322 Å (see also ESI†) and rather short when compared to the data of **2a**. However, note also that the complexes $[Rh(C_2H_4)(H_2O)\{MeC(CH_2PPh_2)_3\}]$ [C–C: 1.406(11) Å] and $[Rh(C_2H_4)(\eta^5{:}\eta^1\text{-}C_5H_4(CH_2)_2PPh_2)]$ [C–C: 1.402(9) Å] were assigned as Rh(I) complexes based on their molecular structures in the solid state.[89,90]

When the rhodium hydrido complex $[Rh(H)(PEt_3)_3]$ (**3**) in benzene was treated with 3,3,3-trifluoropropene in the presence of NEt_3 and Cs_2CO_3 a different reaction pathway was observed (Schemes 1 and 2). The base combination is used for trapping traces of HF, whereas the amine is a phase-transfer agent. At room temperature the reaction led to the activation of the C–F bond of the trifluoromethyl group of the fluorinated olefin to afford the fluorido complex $[Rh(F)(PEt_3)_3]$ (**4**) as well as 1,1-difluoro-1-propene.[63,91] When the reaction was carried out without the presence of a base, the formation of the literature known rhodium bifluoride complex $[Rh(FHF)(PEt_3)_3]$ was also observed as a minor product in a ratio of **4** : $[Rh(FHF)(PEt_3)_3]$ of 3 : 1.[84] The formation of **4** and 1,1-difluoro-1-propene from **3** and 3,3,3-trifluoropropene was also monitored by NMR spectroscopy at low temperature (Scheme 2). The studies revealed the initial generation of *fac*-$[Rh(H)(CH_2CHCF_3)(PEt_3)_3]$ (**5**) at 203 K. The $^{31}P\{^1H\}$ NMR

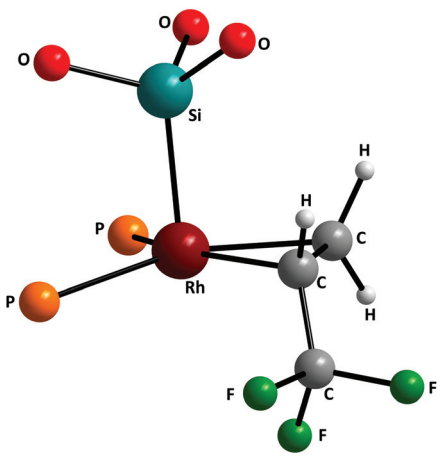

Fig. 1 Part of DFT-optimized structure of the isomer of $[Rh(CH_2CHCF_3)\{Si(OEt)_3\}(PEt_3)_2]$ (**2a**) with the lowest energy. The ethyl groups of the phosphine ligands and the silyl ligand have been omitted for clarity.

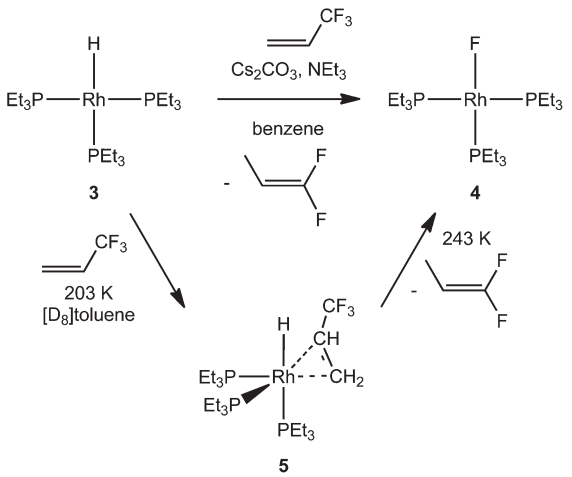

Scheme 2 C–F bond activation of 3,3,3-trifluoropropene at [Rh(H)-(PEt_3)$_3$] (**3**).

spectrum of the reaction solution shows three signals for the three inequivalent phosphine ligands at δ = 18.7, 16.6 and 4.6 ppm an integral ratio of 1 : 1 : 1. The signal patterns are in accordance with a *fac*-configuration for **5**. The doublet of doublet of doublet of doublet of quartets at δ = 18.7 ppm can be assigned to the phosphine ligand in the *trans*-position to the $CHCF_3$ moiety of the fluorinated olefin. The observed splitting pattern is due to the coupling to the rhodium atom ($^1J_{Rh,P}$ = 132 Hz), the coupling to the phosphorous atoms of the other two phosphine ligands ($^2J_{P,P}$ = 33 and $^2J_{P,P}$ = 27 Hz) as well as to coupling to the fluorine atoms of the trifluoromethyl group ($^4J_{P,F}$ = 19 Hz). The inequivalence of the two phosphorus centers *cis* to the hydride ligand is consistent with restricted rotation of the olefin on the NMR time-scale. For the phosphorous atom in *trans*-position to the CH_2-group of the olefin a doublet of doublet of doublets at δ = 16.6 ppm with a comparable rhodium–phosphorous coupling constant of $^1J_{Rh,P}$ = 130 Hz and phosphorous–phosphorous coupling constants of $^2J_{P,P}$ = 33 and $^2J_{P,P}$ = 30 Hz was observed. In contrast, the resonance signal at δ = 4.6 ppm shows a comparable splitting pattern and similar phosphorous–phosphorous coupling constants but a noticeable smaller rhodium–phosphorous coupling constant ($^1J_{Rh,P}$ = 90 Hz), and can therefore be assigned to the phosphorus atom in the *trans*-position to the hydrido ligand. The smaller coupling may be attributed to the large *trans*-influence of the hydrido ligand.[92–95] The $^4J_{P,F}$ = 19 Hz coupling is also observed in a ^{1}H decoupled ^{19}F NMR spectrum, that shows a resonance signal for the CF_3 group at δ = −54.8 ppm which appears as a doublet. The ^{1}H NMR spectrum reveals three resonance signals at δ = 2.65, 2.07 and 1.49 ppm for the hydrogen atoms of the coordinated 3,3,3-trifluoropropene, which is in accordance with the data of the previously reported nickel complex [Ni(CO)($C_3H_3F_3$)(I^tBu)] (I^tBu = *N*,*N*-di(*tert*-butyl)imidazol-2-ylidene).[96] For the metal-bound hydrogen atom the spectrum depicts an apparent doublet of triplets of doublets at δ = −14.36 ppm revealing a large phosphorus–hydrogen coupling of $^2J_{Ptrans,H}$ = 165 Hz to a phosphine ligand in the *trans*-position ($^2J_{Pcis,H} \approx {}^2J_{Pcis,H}$ = 20, $^1J_{Rh,H}$ = 10 Hz). In a ^{31}P NMR decoupling experiment the signal simplifies to a doublet confirming the $^1J_{H,Rh}$ coupling constant.

As above for complex **2**, conceivable rotational isomers of **5** were calculated by DFT. The optimized structures differ in the orientation of the trifluoromethyl group with respect to the hydrido ligand. The computed structure where the trifluoromethyl group points in the same direction as the hydrido ligand seems to be more stable than a *anti*-configuration (Fig. 2). The C–C(CF_3) bond distance with 1.437 Å in **5a** is again noticeable longer when compared to data of the DFT-optimized structure of 3,3,3-trifluoropropene (1.322 Å, see ESI†) but comparable to the distance in the silyl complex [Rh(CH_2CHCF_3){Si(OEt)$_3$}(PEt_3)$_2$] (**2a**).

Treatment of the rhodium germyl complex [Rh($GePh_3$)-(PEt_3)$_3$] (**6**) with 3,3,3-trifluoropropene also gave the fluorido complex **4** by C–F activation as well as the germylated difluoroalkene **7** (Scheme 1).[97] Remarkably, a rare derivatization of the fluorinated substrate was achieved which yielded a new fluorinated building block. Due to the similar solubility properties of complex **4** and the (3,3-difluoroallyl)triphenylgermane **7** in various solvents such as toluene, benzene, pentane or Et_2O, it was not possible to isolate the olefin.

In the ^{19}F NMR spectrum of **7** two resonance signals were observed for the CF_2 unit. A doublet at δ = −90.2 ppm and a doublet of doublets at δ = −92.6 ppm showing a characteristic geminal fluorine–fluorine coupling constant of 50 Hz.[91,98–101] The latter signal can be assigned to the fluorine atom in the *trans*-position to the vinylic proton with a $^3J_{F,H}$ coupling constant of 25 Hz.[91,101–103] The signal for the vinylic proton appears in the ^{1}H NMR spectrum as a doublet of doublet of triplets due to coupling to both fluorine atoms ($^3J_{H,Fcis}$ = 2.4 Hz) as well as to the coupling to the CH_2 group. In the $^{13}C\{^1H\}$ NMR spectrum three resonance signals for the CF_2=$CHCH_2$-moiety were detected. The doublet of doublets at δ = 156.6 ppm can be assigned to the CF_2 group with typical

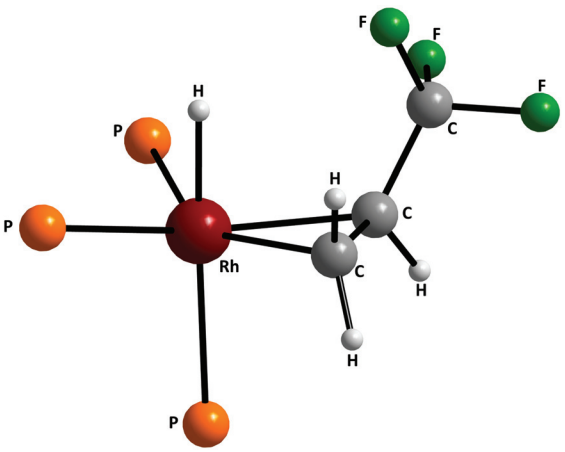

Fig. 2 Part of the DFT-optimized structure of the isomer of *fac*-[Rh(H)(CH_2CHCF_3)(PEt_3)$_3$] (**5a**) with the lowest energy. The ethyl groups of the phosphine ligands have been omitted for clarity.

$^{1}J_{C,F}$ coupling constants of 286.1 and 283.0 Hz. The CH unit also appears as a doublet of doublets at δ = 76.0 ppm but with smaller carbon–fluorine coupling constants ($^{2}J_{C,F}$ = 24.9 and 21.0 Hz). For the CH_2-group a doublet was observed with a C,F coupling ($^{3}J_{C,F}$ = 2.8 Hz). The assignment of the signals was supported by a ^{1}H, ^{13}C HMBC NMR spectrum as well as a ^{19}F, ^{13}C HMBC NMR spectrum (Fig. 3). Suitable crystals for an analysis by X-ray crystallography of the difluoroalkene **7** were obtained on one occasion from the reaction mixture in *n*-hexane at 243 K. The molecular structure in the solid state is illustrated in Fig. 4 and selected bond lengths and angles are summarized in Table 1. Compound **7** crystalizes in the triclinic space group $P\bar{1}$. The C2–C3 bond distance is with 1.291(2) Å rather short compared to the respective separations in other difluoroalkenes like CF_2═CHR [R = H 1.305(1) Å); R = F 1.307 (1) Å; R = CF═CF_2 1.318 (3) Å; R = CH═CF_2 1.321(1) Å][101,104,105] but is in the same range as the ones for germylated fluoroolefins such as $Ph_3GeCF{=}CF_2$ (1.230(8) Å),[98] $Ph_3GeCCl{=}CF_2$ (1.300(8) Å),[99] $Ph_3GeCF{=}CFCF_3$ (1.321(8) Å).[106] The F1–C3–F2 angle is with 107.45(15)° noticeable smaller than 120° but in good accordance to the data for the previously mentioned difluoroalkenes.[105] The torsion angle Ge1–C1–C2–C3 is 115.67°.

Mechanistically it is likely that after a precoordination of the 3,3,3-trifluoropropene at the rhodium(I) complexes **3** or **6** an insertion of the fluorinated olefin into the metal–E (E = H, Ge) bond occurs which is followed by an *β*-fluorine elimination yielding the fluorido complex and the difluoroalkene (Scheme 3). Presumably this involves a phosphine dissociation prior to the *β*-fluorine elimination followed by an association of PEt_3. Jones *et al.* and Lentz and co-workers also described *β*-fluorine elimination reactions at low valent early transition-metal complexes such as [$Cp^*_2Zr(H)(X)$] (X = H, F) or [$Cp_2Ti(F)_2$].[63,65,70,72,73,107]

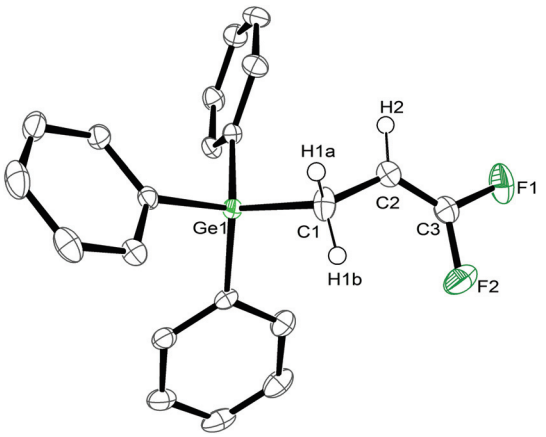

Fig. 4 Molecular structure of **7** (ORTEP diagram). Ellipsoids are drawn at 50% probability level. C–H hydrogen atoms of the phenyl groups were omitted for clarity.

Table 1 Selected bond lengths [Å] and angles [°] in **7**

Lengths [Å]			
Ge1–C1	1.9764(16)	C3–F1	1.327(2)
C1–C2	1.496(2)	C3–F2	1.316(2)
C2–C3	1.291(2)		
Angles [°]			
Ge1–C1–C2	115.64(12)	C2–C3–F2	126.33(17)
C1–C2–C3	125.63(17)	F1–C3–F2	107.45(15)
C2–C3–F1	126.21(17)		

In general, examples for the transition-metal mediated activation of fluorinated alkyl groups are rare, but as mentioned above, most impart alkyl groups at fluorinated olefins or aromatics and result in the formation of cross-coupling or hydrodefluorination products.[51,53,59,63,73,108–117] Note that by

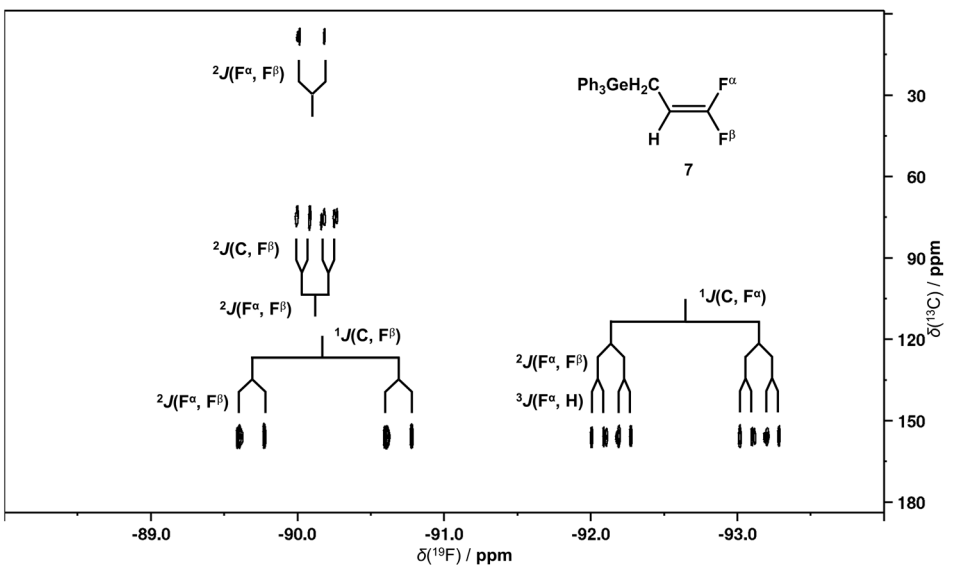

Fig. 3 ^{19}F, ^{13}C HMBC NMR spectrum (282.4 MHz/75.4 MHz, C_6D_6) of (3,3-difluoroallyl)triphenylgermane **7**.

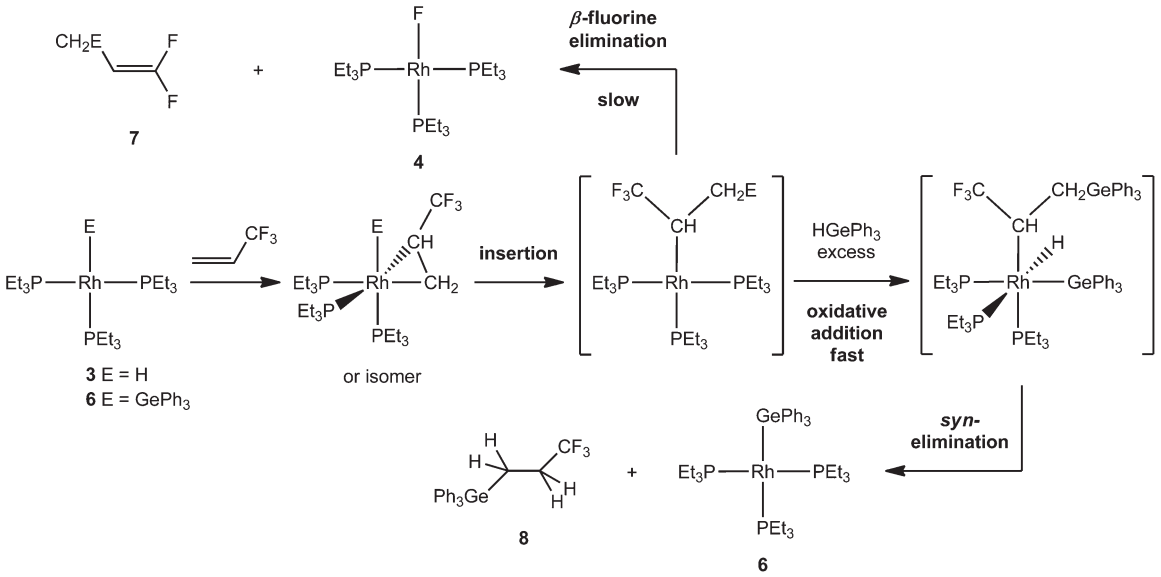

Scheme 3 Possible mechanisms for the C–F bond activation reaction and hydrogermylation of 3,3,3-trifluoropropene.

employing various Lewis acids the cleavage of tertiary C–F bonds can also be induced.[118–135] As mentioned above C–F bond functionalizations to access new fluorinated building blocks include C–C coupling, hydrodefluorination, silylation and borylation reactions.[80] However, a catalytic conversion of 3,3,3-trifluoropropene with $HGePh_3$ in the presence of the germyl complex **6** did not lead to (3,3-difluoroallyl)triphenylgermane **7**. Instead, complex **6** catalyzes a selective hydrogermylation of 3,3,3-trifluoropropene under mild conditions and in good yield. On using 2 mol% of **6** a full conversion of $HGePh_3$ was observed according to the NMR spectra after 6 h at room temperature (TON 38). The 1,1,1-trifluoropropane-3-triphenylgermane **8** was isolated with a yield of 73% corresponding to a TON of 35 based on the amount of triphenylgermane that was employed. Note that the blank test in absence of **6** revealed the formation of **8** in traces (yield 4.6%) after 6 h at room temperature. The germane **8** was characterized by NMR spectroscopy, X-ray crystallography analysis and elemental analysis (Scheme 4). The ^1H NMR spectrum shows two signals of higher order for the methylene groups at 2.08 and 1.56 ppm. The signals can be simulated as AA′ and BB′ parts of an AA′BB′X_3 spin system (Fig. 5).[136]

Suitable crystals for a X-ray crystallography analysis of the hydrogermylation product **8** were obtained after recrystallization in *n*-hexane by slow evaporation of the solvent from a saturated heptane solution at room temperature. The molecular structure of the germane in the solid state is illustrated in Fig. 6 and selected bond lengths and angles are summarized in Table 2. Compound **8** crystalizes in the monoclinic space group $P2_1/c$. The Ge1–C3 bond distance is with 1.966(4) Å comparable to the one in the difluoroalkene **7**. The C–C bond lengths C1–C2 [1.492(6) Å] and C2–C3 [1.519(6) Å] are in a typical range for single bonds. The torsion angle

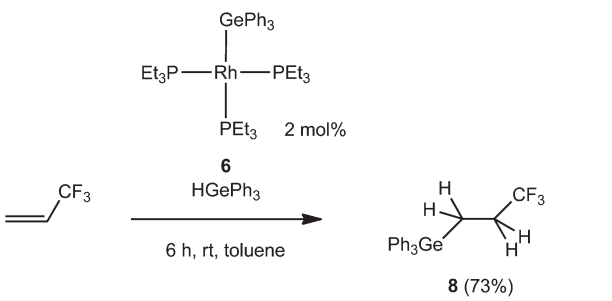

Scheme 4 Rhodium-catalyzed hydrogermylation of 3,3,3-trifluoropropene.

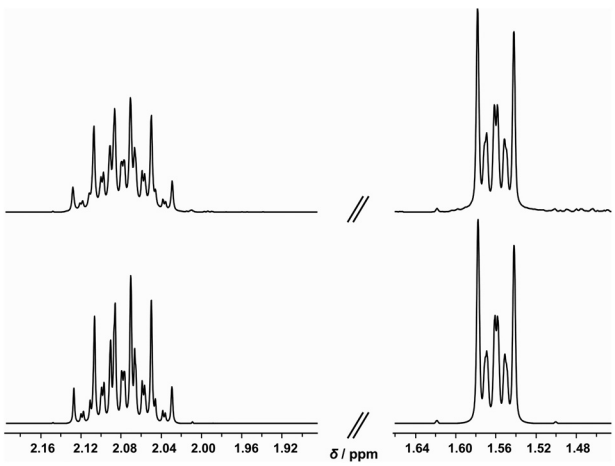

Fig. 5 Part of the ^1H NMR (500.1 MHz, [D_6]benzene) spectrum of $Ph_3GeCH_2CH_2CF_3$ (**8**); simulated (bottom) observed (top) using the following coupling constants (Hz): $^2J(H^a,H^{a'})$ = 14.98, $^3J(H^a,H^b)$ = 13.67, $^3J(H^a,H^{b'})$ = 4.38, $^3J(H^a,F)$ = 10.69, $^3J(H^{a'},H^b)$ = 3.79, $^3J(H^{a'},H^{b'})$ = 13.98, $^3J(H^{a'},F)$ = 9.89, $^2J(H^b,H^{b'})$ = 13.76, $^4J(H^b,F)$ = 0.65 and $^4J(H^{b'},F)$ = 0.25.

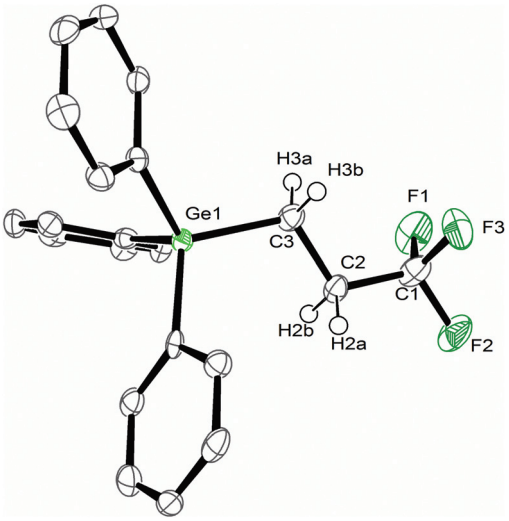

Fig. 6 Molecular structure of **8** (ORTEP diagram). Ellipsoids are drawn at the 50% probability level. C–H hydrogen atoms of the phenyl groups were omitted for clarity.

Table 2 Selected bond lengths [Å] and angles [°] in **8**

Lengths [Å]			
C1–C2	1.492(6)	F1–C1	1.339(5)
C2–C3	1.519(6)	F2–C1	1.341(5)
Ge1–C3	1.966(4)	F3–C1	1.343(5)
Angles [°]			
Ge1–C3–C2	112.6(3)	C1–C2–C3	112.8(4)

C1–C2–C3–Ge1 with 176.30° exemplifies an antiperiplanar conformation of the $GePh_3$ group and the CF_3 group. In contrast to the mechanism mentioned above for the C–F bond activation of the fluorinated olefin at the germyl complex **6** a different reaction pathway becomes feasible in the presence of an excess $HGePh_3$ when the reaction is carried out under catalytic conditions (Scheme 3). After the insertion of the 3,3,3-trifluoropropene into the rhodium–germanium bond an oxidative addition of $HGePh_3$ which is followed by the reductive elimination of 1,1,1-trifluoropropane-3-triphenylgermane appears to be faster than the *β*-fluorine elimination pathway.

To expand the scope of the hydrogermylation reaction $HGeEt_3$ and $HGe(n\text{Bu})_3$ were also employed for the transformation of 3,3,3-trifluoropropene into trifluoropropylgermanes with **6** as catalyst (Scheme 5). However, the conversions were less selective and the formation of 1,1,1-trifluoropropane as a minor product was also observed, and for both germanes longer reaction times are required at room temperature. At 50 °C the TONs are noticeable lower compared to the reaction of $HGePh_3$. After a period of 6 h the NMR spectroscopic measurements of the reaction solutions did not show any further growth of the signals of the products. Note that in these conversions traces of **7** were also generated. For $HGePh_3$ no oxidative addition of the germane at **6** was observed by NMR spectroscopy. However, in the case of $HGeEt_3$ and $HGe(n\text{Bu})_3$ an initial oxidative addition at the Rh(I) germyl compound **6** seems to be active and this opens up pathways for dehydrogermylation reactions and the generation of complex **3**. The formation of digermanes was supported by GC-MS measurements. Intermediate rhodium hydrido complexes $[Rh(H)(PEt_3)_n]$ (n = 3, 4) and tertiary germanes can thus serve as sources for hydrogen resulting in hydrogenation reactions of 3,3,3-trifluoropropene affording 1,1,1-trifluoropropane as a minor product.[62]

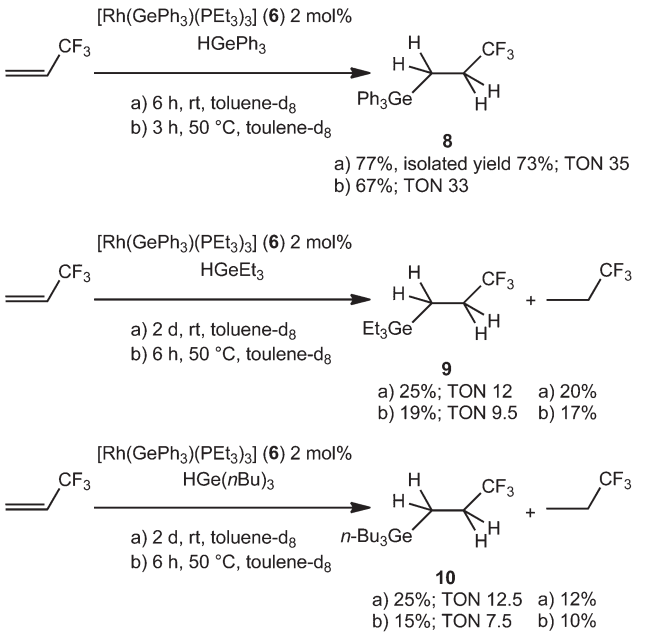

Scheme 5 Scope of the hydrogermylation reaction with different germanium hydrides.

Hydrogermylation reactions of olefins and alkynes have been described, but in contrast to comparable silylation reactions examples are limited.[137–141] Hydrogermylation reactions can also proceed *via* radical pathways and can be initiated by additives, photochemically as well as thermally, but then are often not selective.[137,142–147] However, transition-metal mediated hydrogermylations have also been reported.[146,148–158] Recently, Blanchard and co-workers established a stereoselective hydrogermylation of α-trifluoromethylated alkynes and employed the germylated compounds in subsequent cross-coupling reactions.[158] Note that hydrosilylation reactions of 3,3,3-trifluoropropene with $HSiPh_3$ yielding 1,1,1-trifluoropropane-3-triphenylsilane were described before using $[Rh(H)(PEt_3)_4]$ as a catalyst.[78]

Conclusions

In conclusion we have reported on rhodium-mediated activation reactions of 3,3,3-trifluoropropene. At $[Rh\{Si(OEt)_3\}(PEt_3)_3]$ (**1**), $[Rh(H)(PEt_3)_3]$ (**3**) or $[Rh(GePh_3)(PEt_3)_3]$ (**6**) coordination, hydrodefluorination, or C–F bond activation and concomitant germylation were observed, respectively. The latter two routes are accompanied by a double bond migration to generate

fluoropropenes with a geminal configuration of the fluorine atoms, whereas the reaction of $[Rh\{Si(OEt)_3\}(PEt_3)_3]$ (**1**) with 3,3,3-trifluoropropene is less selective, but there are some indications for a C–F bond cleavage. Note that the structurally related boryl complex $[Rh(Bpin)(PEt_3)_3]$ does react on a stoichiometric scale, but the conversion is not selective and the products were not identified. However, on a catalytic scale the C–F bond activation reaction at **6** seems to be slower than a competing hydrogermylation. Therefore **6** can be employed as a catalyst for hydrogermylation reactions. Comparable rhodium-catalyzed hydrosilylation reactions of 3,3,3-trifluoropropene have been reported.[78] In future work the germylated products might be employed in cross-coupling reactions. Note that Hoge and coworkers recently demonstrated that various tris(pentafluoroethyl)germanes are suitable precursors for ionic compounds.[159–161]

Experimental

General methods and instrumentations

The synthetic work was carried out with a Schlenk line or in a glove box under an atmosphere of argon. All solvents were purified and dried by conventional methods and distilled under an atmosphere of argon before use. $[D_6]$Benzene, $[D_8]$thf and $[D_8]$toluene were dried by stirring over Na/K and then distilled. Triphenylgermane and 3,3,3-trifluoropropene were obtained from ABCR, triethylgermane and tri-*n*-butylgermane from Alfa Aesar. All germanes were used without further purification. $[Rh\{Si(OEt)_3\}(PEt_3)_3]$ (**1**), $[Rh(H)(PEt_3)_3]$ (**3**) and $[Rh(GePh_3)(PEt_3)_3]$ (**6**) were prepared according to the literature.[85,95,97,162] The NMR spectra were acquired on a Bruker DPX 300, Bruker Avance 300 or Bruker Avance 400 spectrometer. The ^{1}H and ^{13}C NMR chemical shifts were referenced to residual $[D_5]$benzene at δ = 7.15 ppm, $[D_7]$thf at δ = 1.73 ppm or $[D_7]$toluene at δ = 2.09 ppm. The ^{19}F NMR spectra were referenced to external $CFCl_3$ at δ = 0.0 ppm. The $^{31}P\{^1H\}$ NMR spectra were referenced externally to 85% H_3PO_4 at δ = 0.0 ppm. $^{29}Si\{^1H\}$ NMR spectra were referenced externally to $Si(CH_3)_4$ at δ = 0.0 ppm. Microanalyses were measured with a HEKAtech Euro EA 3000 elemental analyzer. GC MS analyses were performed with a Shimadzu GCMS-QP2010SE equipped with a Shimadzu Rtx®-5MS column. The yield of the hydrogermylation products **8**, **9** and **10** were determined from ^{19}F NMR spectra by integration of product resonances *versus* the external standard $C_6H_5CF_3$ and are based on the amount of $HGeR_3$ (Et, *n*Bu, Ph) that was employed [TON = amount of $RGeCH_2CH_2CF_3$ (R = Et, *n*Bu, Ph) (mol)/amount of rhodium complex (mol)].

Formation of $[Rh(CH_2CHCF_3)\{Si(OEt)_3\}(PEt_3)_2]$ (2). A solution of $[Rh\{Si(OEt)_3\}(PEt_3)_3]$ (**1**) (25 mg, 53 μmol) in $[D_8]$toluene (0.5 mL) in a Young NMR tube equipped with a PFA inliner was cooled to 77 K, degassed *in vacuo*, and pressurized with 3,3,3-trifluoropropene to 1 atm. After warming up to room temperature the NMR spectroscopic data of the reaction mixture revealed the complete conversion of **1** into **2** as well as the generation of free PEt_3. Analytical data for $[Rh(CH_2CHCF_3)\{Si(OEt)_3\}(PEt_3)_2]$ (**2**): **^{1}H NMR** (300.1 MHz, $[D_8]$toluene): δ = 3.64 (q, ^3J(H,H) = 6.7 Hz, 6H; $SiOCH_2CH_3$), 2.36 (m, dd in the $^1H\{^{31}P\}$NMR spectrum J = 9.3, J = 5.4 Hz, 1H; =CH_2), 2.04 (m, 1H; =CH_2), 1.93–1.72 (m, 12H; PCH_2CH_3), 1.42 (m, 1H; =C*H*), 1.07 (t, ^3J(H,H) = 6.7 Hz, 9H; $SiOCH_2CH_3$), 1.04 (m, t in the $^1H\{^{31}P\}$NMR spectrum, ^3J(H,H) = 7.5 Hz, 9H; PCH_2CH_3), 0.94 (t, ^3J(H,H) = 7.6 Hz, 9H; PCH_2CH_3) ppm. **^{19}F NMR** (282.4 MHz, $[D_8]$toluene): δ = −53.4 (m, d in the $^{19}F\{^1H\}$NMR spectrum ^4J(P,F) = 19 Hz, 3F; CF_3) ppm. **$^{31}P\{^1H\}$ NMR** (121.5 MHz, $[D_8]$ toluene): δ = 20.5 (ddq, ^1J(Rh,P) = 135, ^2J(P,P) = 29, ^4J(P,F) = 19 Hz, 1P), 19.3 (dd, ^1J(Rh,P) = 137 Hz, ^2J(P,P) = 29 Hz, 1P) ppm. **^{1}H,^{29}Si HMBC NMR** (300.1/59.6 MHz, $[D_8]$toluene) δ: 3.7/−49 ($SiOCH_2CH_3$), 2.4/−49 (=CH_2/$SiOCH_2CH_3$), 1.1/−49 ($SiOCH_2CH_3$) ppm.

Formation of *fac*-$[Rh(H)(CH_2CHCF_3)(PEt_3)_3]$ (5). 3,3,3-Trifluoropropene was bubbled for 30 s into a solution of $[Rh(H)(PEt_3)_3]$ (**3**) (20 mg, 0.044 mmol) in $[D_8]$toluene (0.5 mL) at 203 K. After five min the low-temperature NMR spectroscopic data revealed the quantitative the formation of *fac*-$[Rh(H)(CH_2CHCF_3)(PEt_3)_3]$ (**5**). Analytical data for *fac*-$[Rh(H)(CH_2CHCF_3)(PEt_3)_3]$ (**5**): **^{1}H NMR** (300.1 MHz, $[D_8]$ toluene, 218 K): δ = 2.65 (s, br; m in the $^1H\{^{31}P\}$ NMR spectrum, 1H; C*H*), 2.07 (m, d in the $^1H\{^{31}P\}$ NMR spectrum, J = 10 Hz, 1H; C*H*), 1.74 (ddq, dq in the $^1H\{^{31}P\}$ NMR spectrum, ^2J(H,H) = 14, ^2J(P,H) = 8, ^3J(H,H) = 7 Hz, 3H; PCH_2CH_3), 1.55 (ddq, dq in the $^1H\{^{31}P\}$ NMR spectrum, ^2J(H,H) = 14, ^2J(P,H) = 8, ^3J(H,H) = 7 Hz, 3H; PCH_2CH_3 *trans* to $CHCF_3$), 1.46 (ddq, dq in the $^1H\{^{31}P\}$ NMR spectrum, ^2J(H,H) = 14, ^2J(P,H) = 8, ^3J(H, H) = 7 Hz, 7H; PCH_2CH_3, PCH_2CH_3 *trans* to the $CHCF_3$, C*H*), 1.12 (m, 6H; PCH_2CH_3 *trans* to RhH), 1.08 (td, t in the $^1H\{^{31}P\}$ NMR spectrum, ^3J(P,H) = 13, ^3J(H,H) = 7 Hz, 9H; PCH_2CH_3), 0.98 (td, t in the $^1H\{^{31}P\}$ NMR spectrum, ^3J(P,H) = 13, ^3J(H,H) = 7 Hz, 9H; PCH_2CH_3 *trans* to $CHCF_3$), 0.81 (td, t in the $^1H\{^{31}P\}$ NMR spectrum, ^3J(P,H) = 13, ^3J(H,H) = 7 Hz, 9H; PCH_2CH_3 *trans* to RhH), −14.36 (dtd, d in the $^1H\{^{31}P\}$ NMR spectrum, $^2J(P_{trans},H)$ = 165, $^2J(P_{cis},H)$ = $^2J(P_{cis},H)$ = 20, ^1J(Rh, H) = 10 Hz, 1H; Rh*H*) ppm. The assignment of the signals is supported by a ^{1}H, ^{1}H COSY NMR spectrum and a ^{1}H, ^{31}P HMBC NMR spectrum. Note the overlap of the signal for the hydrogen atom of the $CHCF_3$ with a signal of the protons of the phosphine ligand. **^{19}F NMR** (282.4 MHz, $[D_8]$toluene, 203 K): δ = −54.8 (m, d in the $^{19}F\{^1H\}$ NMR spectrum, J(P,F) = 19 Hz; CF_3) ppm. **$^{31}P\{^1H\}$ NMR** (161.9 MHz, $[D_8]$toluene, 203 K): δ = 18.7 (dddq, ^1J(Rh,P) = 132, ^2J(P,P) = 33, ^2J(P,P) = 27, ^4J(P,F) = 19 Hz, 1P; P *trans* to $CHCF_3$), 16.6 (ddd, ^1J(Rh,P) = 130, ^2J(P,P) = 33, ^2J(P,P) = 30 Hz, 1P), 4.6 (ddd, ^1J(Rh,P) = 90, ^2J(P,P) = 30, ^2J(P,P) = 27 Hz, 1P; P *trans* to RhH) ppm.

Reaction of 3,3,3-trifluoropropene with $[Rh(H)(PEt_3)_3]$ (3). To a solution of $[Rh(H)(PEt_3)_3]$ (**3**) (150 mg, 0.327 mmol) in benzene (10 mL) NEt_3 (140 μL, 1.006 mmol) and Cs_2CO_3 (330 mg, 1.013 mmol) were added. 3,3,3-Trifluoropropene was then bubbled for 30 s into the reaction solution. The NMR spectroscopic data of the reaction mixture reveals the formation of 1,1-difluoropropene and $[Rh(F)(PEt_3)_3]$ (**4**). All volatiles were removed in vacuum and the residue was extracted

with *n*-hexane (3 × 3 mL). The solvent was removed from the extract in vacuum. The NMR spectroscopic data of the residue reveals the formation of $[Rh(F)(PEt_3)_3]$ (**4**) (90%). Complex **4** and 1,1-difluoropropene were identified by comparison of their analytical data with the literature.[62,64,84]

Reaction of 3,3,3-trifluoropropene with $[Rh(GePh_3)(PEt_3)_3]$ (6). In a Young NMR tube $[Rh(GePh_3)(PEt_3)_3]$ (**6**) (17 mg, 22.3 μmol) was dissolved in [D$_8$]toluene (0.3 mL). The solution was cooled to 77 K, degassed *in vacuo*, and pressurized with 3,3,3-trifluoropropene to 1 atm. After warming up to room temperature the NMR spectroscopic data of the reaction mixture revealed after 4 h the complete conversion of **6** into $[Rh(F)(PEt_3)_3]$ (**4**) as well as the formation of (3,3-difluoroallyl)-triphenylgermane **7**. Complex **4** was identified by comparison of its analytical data with the literature.[62,64,84] Analytical data for **7**: **^{1}H NMR** (300.1 MHz, [D$_6$]benzene): δ = 7.44 (m, 6H; Ph), 7.18 (m, 9H; Ph), 4.15 (ddt, ^3J(H,F$^\alpha$) = 24.7, ^3J(H,H) = 8.8, ^3J(H,F$^\beta$) = 2.4 Hz, 1H; C*H*), 1.98 (dt, ^3J(H,H) = 8.8, ^4J(H,F) = 1.7 Hz, 2H; CH_2) ppm. **^{13}C{^{1}H} NMR** (75.5 MHz, [D$_8$]thf): δ = 156.6 (dd, ^1J(C,F$^\alpha$) = 286.1, ^1J(C,F$^\beta$) = 283.0 Hz; *C*F$_2$), 136.8 (s, Ph), 135.5 (s, Ph), 129.9 (s, Ph), 129.1 (s, Ph), 76.0 (dd, ^2J(C,F$^\beta$) = 24.9, ^2J(C,F$^\alpha$) = 21.0 Hz; CH), 8.6 (d, ^3J(C,F) = 2.8 Hz; CH$_2$) ppm, the assignment of the signals is supported by a ^{1}H, ^{13}C HMBC NMR spectrum as well as a ^{19}F, ^{13}C{^{1}H} HMBC NMR spectrum. **^{19}F NMR** (282.4 MHz, [D$_8$]thf): δ = −90.2 (d, ^2J(F,F) = 50 Hz, 1F; F$^\beta$), −92.6 (dd, ^2J(F,F) = 50, ^3J(F,H) = 25 Hz, 1F; F$^\alpha$) ppm (for the labeling of the fluorine atoms see also Scheme 1).

Treatment of $HGePh_3$ with 3,3,3-trifluoropropene. In a Young NMR tube $HGePh_3$ (60 mg, 196 μmol) was dissolved in [D$_8$]toluene (0.4 mL). The solution was cooled to 77 K, degassed *in vacuo*, and pressurized with 3,3,3-trifluoropropene to 1 atm. After warming up to room temperature the reaction solution was monitored by NMR spectroscopy. After 6 h the ^{19}F NMR spectroscopic data revealed the formation of $Ph_3GeCH_2CH_2CF_3$ (**7**) (4.6%).

Catalytic conversion of 3,3,3-trifluoropropene with $HGePh_3$. (a) In a Young NMR tube $[Rh(GePh_3)(PEt_3)_3]$ (**6**) (5.5 mg, 7.22 μmol) was dissolved in [D$_8$]toluene (0.3 mL) and $HGePh_3$ (110 mg, 360 μmol) was added to the solution. The solution was cooled to 77 K, degassed *in vacuo*, and pressurized with 3,3,3-trifluoropropene to 1 atm. After warming up to room temperature the reaction was monitored by NMR spectroscopy. After 6 h at room temperature the ^{1}H and ^{19}F NMR spectroscopic data reveal the complete conversion of $HGePh_3$ as well as the formation of $Ph_3GeCH_2CH_2CF_3$ (**8**) (77%, TON = 38). All volatiles were removed *in vacuo* and the crude product was recrystallized from a saturated solution in *n*-hexane (1.5 mL). **8** was obtained as a colorless solid. Yield 105 mg (73%; TON = 36). (b) In a Young NMR tube $[Rh(GePh_3)(PEt_3)_3]$ (**6**) (5.5 mg, 7.22 μmol) was dissolved in [D$_8$]toluene (0.3 mL) and $HGePh_3$ (110 mg, 360 μmol) was added to the solution. The solution was cooled to 77 K, degassed *in vacuo*, and pressurized with 3,3,3-trifluoropropene to 1 atm. After warming up to room temperature the reaction was monitored by NMR spectroscopy. After 3 h at 323 K the ^{1}H and ^{19}F NMR spectroscopic data reveal the complete conversion of $HGePh_3$ as well as the formation of **8** (67%; TON = 33). Analytical data for $Ph_3GeCH_2CH_2CF_3$ (**8**): $C_{21}H_{19}F_3Ge$ (401.01): calcd C, 62.90; H, 4.78; found: C, 63.31; H, 4.86. **^{1}H NMR** (500.1 MHz, [D$_6$]benzene): δ = 7.33 (m, 6H; Ph), 7.14–7.09 (m, 9H; Ph) 2.08 (m, ^2J(H^a,H$^{a'}$) = 14.98, ^3J(H^a,H^b) = 13.67, ^3J(H^a,H$^{b'}$) = 4.38, ^3J(H^a,F) = 10.69, ^3J(H$^{a'}$,H^b) = 3.79, ^3J(H$^{a'}$,H$^{b'}$) = 13.98, ^3J(H$^{a'}$,F) = 9.89 Hz, 2H; CH_2), 1.56 (m, ^3J(H^a,H^b) = 13.67, ^3J(H^a,H$^{b'}$) = 4.38, J(H$^{a'}$,H^b) = 3.79, ^3J(H$^{a'}$,H$^{b'}$) = 13.98, ^4J(H^b,F) = 0.65 ^4J(H$^{b'}$,F) = 0.25 Hz, 2H; CH_2GePh$_3$) ppm. The coupling constants were determined by simulation with gNMR.[136] **^{13}C{^{1}H} NMR** (75.5 MHz, [D$_8$]thf): δ = 136.3 (s, Ph), 135.4 (s, Ph), 129.8 (s, Ph), 129.0 (s, Ph) 128.6 (q, ^1J(C,F) = 276 Hz; CF$_3$), 30.3 (q, ^2J(C,F) = 30 Hz; CH$_2$), 5.9 (q, ^3J(C,F) = 2 Hz; CH$_2$GePh$_3$) ppm, the assignment of the signals is supported by a ^{19}F,^{13}C{^{1}H} HMBC NMR spectrum (see also ESI†). **^{19}F NMR** (282.4 MHz, [D$_8$]thf): δ = −71.2 (t, ^3J(F,H) = 10 Hz, 3F; CF$_3$) ppm.

Catalytic conversion of 3,3,3-trifluoropropene with $HGeEt_3$. (a) In a Young NMR tube $[Rh(GePh_3)(PEt_3)_3]$ (**6**) (5.5 mg, 7.22 μmol) and $HGeEt_3$ (58 μL, 0.361 mmol) were dissolved in [D$_8$]toluene (0.3 mL). The solution was cooled to 77 K, degassed *in vacuo*, and pressurized with 3,3,3-trifluoropropene to 1 atm. After warming up to room temperature the reaction was monitored by NMR spectroscopy. After 2 d at room temperature the ^{1}H and ^{19}F NMR spectroscopic data reveal the formation of $Et_3GeCH_2CH_2CF_3$ (**9**) (25%; TON = 12) as well as of 1,1,1-trifluoropropane (20%). $Et_3GeGeEt_3$ was identified as a minor product by comparison with literature data and by GC-MS analysis of the reaction mixtures.[163] (b) In a Young NMR tube $[Rh(GePh_3)(PEt_3)_3]$ (**6**) (6.6 mg, 8.60 μmol) and $HGeEt_3$ (70 μL, 0.433 mmol) were dissolved in [D$_8$]toluene (0.3 mL). The solution was cooled to 77 K, degassed *in vacuo*, and pressurized with 3,3,3-trifluoropropene to 1 atm. After warming up to 323 K the reaction was monitored by NMR spectroscopy. After 6 h the ^{1}H and ^{19}F NMR spectroscopic data reveal the formation of $Et_3GeCH_2CH_2CF_3$ (**9**) (19%; TON = 12) as well as of 1,1,1-trifluoropropane (17%). Analytical data for **9**: **^{1}H NMR** (500.1 MHz, [D$_8$]toluene): δ = 1.84 (m, 2H; CH_2CF$_3$), 0.88 (t, ^3J(H,H) = 8 Hz, 9H, GeCH$_2$CH_3), 0.74 (m, 2H; CH_2), 0.53 (q, ^3J(H,H) = 8 Hz, 6H; GeCH_2CH$_3$) ppm, the assignment of the signals is supported by a ^{1}H,^{13}C HMBC NMR spectrum as well as a ^{1}H,^{13}C HMQC NMR spectrum. **^{13}C{^{1}H} NMR** (128.4 MHz, [D$_8$]toluene): δ = 128.6 (q, ^1J(C,F) = 277 Hz; CF$_3$), 30.3 (q, ^2J(C,F) = 30 Hz; *C*H$_2$CF$_3$), 8.9 (s, Ge*C*H$_2$CH$_3$), 5.9 (q, ^3J(C,F) = 2 Hz; *C*H$_2$GeEt$_3$), 3.8 (s; GeCH$_2$*C*H$_3$) ppm, the assignment of the signals is supported by a ^{1}H, ^{13}C HMBC NMR spectrum as well as a ^{19}F, ^{13}C{^{1}H} HMBC NMR spectrum. **^{19}F NMR** (282.4 MHz, [D$_8$]toluene): δ = −68.9 (t, ^3J(F,H) = 10 Hz, 3F; CF$_3$) ppm. **GC/MS**: *m*/*z* 229 [M − Et].

Catalytic conversion of 3,3,3-trifluoropropene with HGe(*n*Bu)$_3$. In a Young NMR tube $[Rh(GePh_3)(PEt_3)_3]$ (**3**) (6.0 mg, 7.88 μmol) and HGe(*n*Bu)$_3$ (91 μL, 0.394 mmol) were dissolved in [D$_8$]toluene (0.3 mL). The solution was cooled to 77 K, degassed *in vacuo*, and pressurized with 3,3,3-trifluoropropene to 1 atm. After warming up to room temperature the reaction was monitored by NMR spectroscopy. After 2 d at room temp-

erature the ^{1}H and ^{19}F NMR spectroscopic data reveal the formation of $(n\text{Bu})_3\text{GeCH}_2\text{CH}_2\text{CF}_3$ (**10**) (25%; TON = 12) as well as of 1,1,1-trifluoropropane (12%). $(n\text{Bu})_3\text{GeGe}(n\text{Bu})_3$ was identified as side product by comparison with literature data and by GC-MS analysis of the reaction mixtures.[164] (b) In a Young NMR tube $[\text{Rh}(\text{GePh}_3)(\text{PEt}_3)_3]$ (**3**) (5.2 mg, 6.83 μmol) and $\text{HGe}(n\text{Bu})_3$ (80 μL, 0.340 mmol) were dissolved in $[\text{D}_8]$toluene (0.3 mL). The solution was cooled to 77 K, degassed *in vacuo*, and pressurized with 3,3,3-trifluoropropene to 1 atm. After warming up to 323 K the reaction was monitored by NMR spectroscopy. After 6 h the ^{1}H and ^{19}F NMR spectroscopic data reveal the formation of $(n\text{Bu})_3\text{GeCH}_2\text{CH}_2\text{CF}_3$ (**10**) (15%; TON = 7.5) as well as of 1,1,1-trifluoropropane (10%). Analytical data for **10**: **^{1}H NMR** (300.1 MHz, $[\text{D}_8]$toluene): δ = 1.91 (m, 2H; $\text{C}H_2\text{CF}_3$), 1.28 (m, 12H; CH_2), 0.90 (t, 9H; CH_3), 0.80 (m, 2H; CH_2), 0.61 (m, 6H; CH_2) ppm, the assignment of the signals is supported by a ^{1}H, ^{13}C HMBC NMR spectrum as well as a ^{1}H, ^{13}C HMQC NMR spectrum. **^{13}C{^{1}H} NMR** (75.5 MHz, $[\text{D}_6]$benzene): δ = 128.0 (q, ^1J(C,F) = 277 Hz; CF_3), 29.9 (q, ^2J(C,F) = 29 Hz; CH_2), 27.2 (s, CH_2), 26.5 (s, CH_2), 13.5 (s, CH_2), 11.9 (s, CH_3), 3.7 (q, ^3J(C,F) = 2 Hz; CH_2) ppm, the assignment of the signals is supported by a ^{1}H, ^{13}C HMBC NMR spectrum as well as a ^{19}F, ^{13}C{^{1}H} HMBC NMR spectrum. **^{19}F NMR** (282.4 MHz, $[\text{D}_8]$toluene): δ = −69.0 (t, ^3J(F,H) = 10 Hz, 3F; CF_3) ppm. **GC/MS**: *m*/*z* 285 [M − *n*Bu].

Structure determination

Suitable crystals for X-ray crystallography of (3,3-difluoroallyl)-triphenylgermane **7** were obtained from the reaction mixture of **4** and **7** of a saturated *n*-hexane solution at 243 K. Colorless crystals of 1,1,1-trifluoropropane-3-triphenylgermane **8** were obtained by slow evaporation of the solvent from a *n*-heptane solution at room temperature. Data collections were performed at 100 K with a Bruker D8 Venture area detector. The structures were solved by intrinsic phasing (SHELXS-2013) and refined by full matrix least-squares procedures based on F^2 with all measured reflections (SHELXL-2013).[165–167] The SADABS program was used for multi-scan absorption corrections.[168] All non-hydrogen atoms were refined anisotropically. All hydrogen atom positions were placed at their idealized positions and were refined using a riding model. CCDC 1496566 [for (3,3-difluoroallyl)triphenylgermane **7**] and 1496565 (for 1,1,1-trifluoropropane-3-triphenylgermane **8**) contain the crystallographic data (Table 3).

Computational methods

The calculations were run using the Gaussian 09 (Revision D.01) program package[169] and the B3LYP functional. Plausible ligand arrangements for $[\text{Rh}\{\text{Si}(\text{OEt})_3\}(\text{CH}_2\text{CHCF}_3)(\text{PEt}_3)_2]$ (**2**) and *fac*-$[\text{Rh}(\text{H})(\text{CH}_2\text{CHCF}_3)(\text{PEt}_3)_3]$ (**5**) were optimized and the depicted structures (see Fig. 1 and 2 as well as the ESI†) turned out to be the minima. The cc-pVTZ basis sets were employed for all rhodium- and silicon-bound atoms (cc-pVDZ for all other carbon and hydrogen atoms). Rhodium was described on using RECPs with the associated cc-pVTZ-PP basis set.[170] Frequency calculations were run for all stationary points to identify them as minima (no negative eigenvalues). Energies were corrected for zero-point energy.

Table 3 Crystallographic data

	7	**8**
Crystal dimensions [mm^3]	0.51 × 0.14 × 0.03	0.388 × 0.053 × 0.011
Crystal colour	Colorless	Colorless
Empirical formula	$C_{21}H_{18}F_2Ge$	$C_{21}H_{19}F_3Ge$
M	380.94	400.95
Crystal system	Triclinic	Monoclinic
Space group	$P\bar{1}$	$P2_1/c$
a [Å]	9.4950(4)	16.3551(13)
b [Å]	9.7733(4)	14.7943(10)
c [Å]	10.3171(4)	7.4616(6)
α [°]	67.024(2)	
β [°]	83.103(2)	90.874(3)
γ [°]	84.211(2)	
V [Å^3]	873.54(6)	1805.2(2)
Z	2	4
D_{calcd} [mg m^{-3}]	1.448	1.475
μ(Mo-K$_\alpha$) [mm^{-1}]	1.771	1.726
θ range [°]	2.16 to 28.32	2.49 to 24.55
Reflns. collected	28 469	19 769
Indep. reflns.	4346	3199
R_{int}	0.0351	0.1394
Completeness [%]	99.8	99.7
Absorption correction	Multi-scan	Multi-scan
GoF on F^2	1.052	1.040
R_1, wR_2 (all data)	0.0288, 0.0657	0.0874, 0.0894
R_1, wR_2 ($I_0 > 2$)	0.0261, 0.0643	0.0487, 0.0798
Max. diff. peak/hole [e Å^{-3}]	0.543/−0.392	0.421/−0.409

Acknowledgements

We would like to acknowledge the DFG research training group "Fluorine as a Key Element" (T. Ahrens and M. Teltewskoi) for financial support. M. Ahrens thanks the "Fonds der Chemischen Industrie".

References

1 R. E. Banks, *Fluorine Chemistry at the Millennium: Fascinated by Fluorine*, Elsevier, Amsterdam, 2000.
2 T. Hiyama, *Organofluorine Compounds: Chemistry and Applications*, Springer, Berlin, 2000.
3 P. Kirsch, *Modern Fluoroorganic Chemistry: Synthesis*, Reactivity and Applications, Wiley-VCH Weinheim, 2004.
4 J. A. Gladysz, *Handbook of Fluorous Chemistry*, Wiley-VCH, Weinheim, 2004.
5 J. P. Bégué and D. Bonnet-Delpon, *Bioorganic and Medicinal Chemistry of Fluorine*, John Wiley & Sons, Inc, Hoboken, New York, 2008.
6 Y. Zhou, J. Wang, Z. Gu, S. Wang, W. Zhu, J. L. Aceña, V. A. Soloshonok, K. Izawa and H. Liu, *Chem. Rev.*, 2016, **116**, 422–518.
7 J. L. Kiplinger, T. G. Richmond and C. E. Osterberg, *Chem. Rev.*, 1994, **94**, 373–431.

8 J. Burdeniuc, B. Jedlicka and R. H. Crabtree, *Chem. Ber.*, 1997, **130**, 145–154.
9 T. Richmond, in *Activation of Unreactive Bonds and Organic Synthesis*, ed. S. Murai, Springer, Berlin Heidelberg, 1999, vol. 3, ch. 10, pp. 243–269.
10 T. G. Richmond, *Angew. Chem., Int. Ed.*, 2000, **39**, 3241–3244, (*Angew. Chem.*, 2000, **112**, 3378–3380).
11 T. Braun and R. N. Perutz, *Chem. Commun.*, 2002, 2749–2757.
12 W. D. Jones, *Dalton Trans.*, 2003, 3991–3995.
13 T. Braun and R. N. Perutz, in *Perspectives in Organometallic Chemistry*, ed. C. G. Screttas and B. R. Steele, Royal Soc Chemistry, Cambridge, 2003, pp. 136–151.
14 U. Mazurek and H. Schwarz, *Chem. Commun.*, 2003, 1321–1326.
15 H. Torrens, *Coord. Chem. Rev.*, 2005, **249**, 1957–1985.
16 R. N. Perutz and T. Braun, in *Comprehensive Organometallic Chemistry III*, ed. D. M. P. Mingos and R. H. Crabtree, Elsevier, Oxford, 2007, pp. 725–758.
17 S. A. Macgregor, *Chem. Soc. Rev.*, 2007, **36**, 67–76.
18 R. P. Hughes, *Eur. J. Inorg. Chem.*, 2009, 4591–4606.
19 G. Meier and T. Braun, *Angew. Chem., Int. Ed.*, 2009, **48**, 1546–1548, (*Angew. Chem.*, 2009, **121**, 1575–1577).
20 H. Amii and K. Uneyama, *Chem. Rev.*, 2009, **109**, 2119–2183.
21 A. D. Sun and J. A. Love, *Dalton Trans.*, 2010, **39**, 10362–10374.
22 T. Braun and F. Wehmeier, *Eur. J. Inorg. Chem.*, 2011, 613–625.
23 E. Clot, O. Eisenstein, N. Jasim, S. A. Macgregor, J. E. McGrady and R. N. Perutz, *Acc. Chem. Res.*, 2011, **44**, 333–348.
24 J.-F. Paquin, *Synlett*, 2011, 289–293.
25 S. A. Johnson, J. A. Hatnean and M. E. Doster, *Progress in Inorganic Chemistry*, Wiley, 2011.
26 M. Klahn and U. Rosenthal, *Organometallics*, 2012, **31**, 1235–1244.
27 A. Nova, R. Mas-Balleste and A. Lledos, *Organometallics*, 2012, **31**, 1245–1256.
28 M. Crespo, *Organometallics*, 2012, **31**, 1216–1234.
29 T. Braun, *Organometallics*, 2012, **31**, 1213–1215.
30 L. Keyes and J. A. Love, in *C-H and C-X Bond Functionalization: Transition Metal Mediation*, ed. X. Ribas, The Royal Society of Chemistry, 2013, pp. 159–192.
31 M. F. Kuehnel, D. Lentz and T. Braun, *Angew. Chem., Int. Ed.*, 2013, **52**, 3328–3348, (*Angew. Chem.*, 2013, **125**, 3412–3433).
32 J. Weaver and S. Senaweera, *Tetrahedron*, 2014, **70**, 7413–7428.
33 T. Braun and R. P. Hughes, *Organometallic Fluorine Chemistry*, Springer International Publishing, Switzerland, 2015.
34 For recent catalytic borylation and cross-coupling reactions, see for example ref. 34–46: Q. Shen, Y.-G. Huang, C. Liu, J.-C. Xiao, Q.-Y. Chen and Y. Guo, *J. Fluorine Chem.*, 2015, **179**, 14–22.
35 K. Fuchibe, T. Morikawa, R. Ueda, T. Okauchi and J. Ichikawa, *J. Fluorine Chem.*, 2015, **179**, 106–115.
36 S. I. Kalläne, M. Teltewskoi, T. Braun and B. Braun, *Organometallics*, 2015, **34**, 1156–1169.
37 X.-W. Liu, J. Echavarren, C. Zarate and R. Martin, *J. Am. Chem. Soc.*, 2015, **137**, 12470–12473.
38 H. Luo, G. Wu, S. Xu, K. Wang, C. Wu, Y. Zhang and J. Wang, *Chem. Commun.*, 2015, **51**, 13321–13323.
39 A. Singh, J. J. Kubik and J. D. Weaver, *Chem. Sci.*, 2015, **6**, 7206–7212.
40 J. M. Gadsby, C. B. McPake, C. B. Murray and G. Sandford, *J. Fluorine Chem.*, 2016, **181**, 51–55.
41 S. Senaweera and J. D. Weaver, *J. Am. Chem. Soc.*, 2016, **138**, 2520–2523.
42 J. Zhou, M. W. Kuntze-Fechner, R. Bertermann, U. S. D. Paul, J. H. J. Berthel, A. Friedrich, Z. Du, T. B. Marder and U. Radius, *J. Am. Chem. Soc.*, 2016, **138**, 5250–5253.
43 T. Niwa, H. Ochiai, Y. Watanabe and T. Hosoya, *J. Am. Chem. Soc.*, 2015, **137**, 14313–14318.
44 J. Zhou, J. H. J. Berthel, M. W. Kuntze-Fechner, A. Friedrich, T. B. Marder and U. Radius, *J. Org. Chem.*, 2016, **81**, 5789–5794.
45 J. Li, T. Zheng, H. Sun, W. Xu and X. Li, *Dalton Trans.*, 2013, **42**, 5740–5748.
46 A. Matsunami, S. Kuwata and Y. Kayaki, *ACS Catal.*, 2016, 5181–5185.
47 P. L. Watson, T. H. Tulip and I. Williams, *Organometallics*, 1990, **9**, 1999–2009.
48 W. Heitz and A. Knebelkamp, *Macromol. Rapid Commun.*, 1991, **12**, 69–75.
49 T. Saeki, Y. Takashima and K. Tamao, *Synlett*, 2005, 1771–1774.
50 J. Ichikawa, K. Sakoda, J. Mihara and N. Ito, *J. Fluorine Chem.*, 2006, **127**, 489–504.
51 J. Ichikawa, R. Nadano and N. Ito, *Chem. Commun.*, 2006, 4425–4427.
52 D. J. Anderson, R. McDonald and M. Cowie, *Angew. Chem., Int. Ed.*, 2007, **46**, 3741–3744, (*Angew. Chem.*, 2007, **119**, 3815–3818).
53 M. Ohashi, T. Kambara, T. Hatanaka, H. Saijo, R. Doi and S. Ogoshi, *J. Am. Chem. Soc.*, 2011, **133**, 3256–3259.
54 W. Xu, H. Sun, Z. Xiong and X. Li, *Organometallics*, 2013, **32**, 7122–7132.
55 T. Ichitsuka, T. Fujita, T. Arita and J. Ichikawa, *Angew. Chem., Int. Ed.*, 2014, **53**, 7564–7568, (*Angew. Chem.*, 2014, **162**, 7694–7698).
56 (*a*) P. Tian, C. Feng and T.-P. Loh, *Nat. Commun.*, 2015, **6**, 7472; (*b*) Y. Huang and T. Hayashi, *J. Am. Chem. Soc.*, 2016, **138**, 12340–12343.
57 M. Ohashi and S. Ogoshi, in *Organometallic Fluorine Chemistry*, ed. T. Braun and P. R. Hughes, Springer International Publishing, Cham, 2015, pp. 197–215.
58 K. Kikushima, H. Sakaguchi, H. Saijo, M. Ohashi and S. Ogoshi, *Chem. Lett.*, 2015, **44**, 1019–1021.
59 (*a*) R. Doi, M. Ohashi and S. Ogoshi, *Angew. Chem., Int. Ed.*, 2016, **55**, 341–344, (*Angew. Chem.*, 2016, **128**, 349–

352); (*b*) Z. Zhang, Q. Zhou, W. Yu, T. Li, G. Wu, Y. Zhang and J. Wang, *Org. Lett.*, 2015, **17**, 2474–2477.
60 M. Fujiwara, J. Ichikawa, T. Okauchi and T. Minami, *Tetrahedron Lett.*, 1999, **40**, 7261–7265.
61 L. A. Watson, D. V. Yandulov and K. G. Caulton, *J. Am. Chem. Soc.*, 2001, **123**, 603–611.
62 T. Braun, D. Noveski, B. Neumann and H. G. Stammler, *Angew. Chem., Int. Ed.*, 2002, **41**, 2745–2748, (*Angew. Chem.*, 2002, **114**, 2870–2873).
63 B. M. Kraft and W. D. Jones, *J. Am. Chem. Soc.*, 2002, **124**, 8681–8689.
64 D. Noveski, T. Braun, M. Schulte, B. Neumann and H. G. Stammler, *Dalton Trans.*, 2003, 4075–4083.
65 E. Clot, C. Megret, B. M. Kraft, O. Eisenstein and W. D. Jones, *J. Am. Chem. Soc.*, 2004, **126**, 5647–5653.
66 J. Vela, J. M. Smith, Y. Yu, N. A. Ketterer, C. J. Flaschenriem, R. J. Lachicotte and P. L. Holland, *J. Am. Chem. Soc.*, 2005, **127**, 7857–7870.
67 D. Huang, K. B. Renkema and K. G. Caulton, *Polyhedron*, 2006, **25**, 459–468.
68 R. D. Rieth, W. W. Brennessel and W. D. Jones, *Eur. J. Inorg. Chem.*, 2007, 2839–2847.
69 S. Yamada, T. Takahashi, T. Konno and T. Ishihara, *Chem. Commun.*, 2007, 3679–3681.
70 B. M. Kraft, E. Clot, O. Eisenstein, W. W. Brennessel and W. D. Jones, *J. Fluorine Chem.*, 2010, **131**, 1122–1132.
71 S. Yamada, K. Shimoji, T. Takahashi, T. Konno and T. Ishihara, *Chem. – Asian J.*, 2010, **5**, 1846–1853.
72 M. F. Kuhnel and D. Lentz, *Angew. Chem., Int. Ed.*, 2010, **49**, 2933–2936, (*Angew. Chem.*, 2010, **122**, 2995–2998).
73 M. F. Kuehnel, P. Holstein, M. Kliche, J. Kruger, S. Matthies, D. Nitsch, J. Schutt, M. Sparenberg and D. Lentz, *Chem. – Eur. J.*, 2012, **18**, 10701–10714.
74 M. F. Kuehnel, T. Schloder, S. Riedel, B. Nieto-Ortega, F. J. Ramirez, J. T. L. Navarrete, J. Casado and D. Lentz, *Angew. Chem., Int. Ed.*, 2012, **51**, 2218–2220, (*Angew. Chem.*, 2012, **124**, 2261–2263).
75 H. Zhang, J.-H. Lin, J.-C. Xiao and Y.-C. Gu, *Org. Biomol. Chem.*, 2014, **12**, 581–588.
76 T. Braun, B. Blocker, V. Schorlemer, B. Neumann, A. Stammler and H.-G. Stammler, *J. Chem. Soc., Dalton Trans.*, 2002, 2213–2218.
77 K. Sakoda, J. Mihara and J. Ichikawa, *Chem. Commun.*, 2005, 4684–4686.
78 T. Braun, F. Wehmeier and K. Altenhoener, *Angew. Chem., Int. Ed.*, 2007, **46**, 5321–5324, (*Angew. Chem.*, 2007, **119**, 5415–5418).
79 T. Braun, M. A. Salomon, K. Altenhoner, M. Teltewskoi and S. Hinze, *Angew. Chem., Int. Ed.*, 2009, **48**, 1818–1822, (*Angew. Chem.*, 2009, **121**, 1850–1854).
80 T. Ahrens, J. Kohlmann, M. Ahrens and T. Braun, *Chem. Rev.*, 2015, **115**, 931–972.
81 J.-Y. Hu, J. Zhang, G.-X. Wang, H.-L. Sun and J.-L. Zhang, *Inorg. Chem.*, 2016, **55**, 2274–2283.
82 K. A. Giffin, I. Korobkov and R. T. Baker, *Dalton Trans.*, 2015, **44**, 19587–19596.
83 D. Lanzinger, I. M. Höhlein, S. B. Weiß and B. Rieger, *J. Organomet. Chem.*, 2015, **778**, 21–28.
84 D. Noveski, T. Braun and S. Kruckemeier, *J. Fluorine Chem.*, 2004, **125**, 959–966.
85 A. L. Raza, J. A. Panetier, M. Teltewskoi, S. A. Macgregor and T. Braun, *Organometallics*, 2013, **32**, 3795–3807.
86 A. L. Raza and T. Braun, *Chem. Sci.*, 2015, **6**, 4255–4260.
87 M. Ahijado, T. Braun, D. Noveski, N. Kocher, B. Neumann, D. Stalke and H. G. Stammler, *Angew. Chem., Int. Ed.*, 2005, **44**, 6947–6951, (*Angew. Chem.*, 2005, **117**, 7107–7111).
88 M. Teltewskoi, J. A. Panetier, S. A. Macgregor and T. Braun, *Angew. Chem., Int. Ed.*, 2010, **49**, 3947–3951, (*Angew. Chem.*, 2010, **122**, 4039–4043).
89 D. J. Rauscher, E. G. Thaler, J. C. Huffman and K. G. Caulton, *Organometallics*, 1991, **10**, 2209–2216.
90 I. Lee, F. Dahan, A. Maisonnat and R. Poilblanc, *Organometallics*, 1994, **13**, 2743–2750.
91 V. W. Weiss, P. Beak and W. H. Flygare, *J. Chem. Phys.*, 1967, **46**, 981–988.
92 T. G. Appleton, H. C. Clark and L. E. Manzer, *Coord. Chem. Rev.*, 1973, **10**, 335–422.
93 B. J. Coe and S. J. Glenwright, *Coord. Chem. Rev.*, 2000, **203**, 5–80.
94 L. Zamostna, S. Sander, T. Braun, R. Laubenstein, B. Braun, R. Herrmann and P. Klaering, *Dalton Trans.*, 2015, **44**, 9450–9469.
95 T. Braun, D. Noveski, M. Ahijado and F. Wehmeier, *Dalton Trans.*, 2007, 3820–3825.
96 R. Dorta, E. D. Stevens, N. M. Scott, C. Costabile, L. Cavallo, C. D. Hoff and S. P. Nolan, *J. Am. Chem. Soc.*, 2005, **127**, 2485–2495.
97 T. Ahrens, M. Ahrens, T. Braun, B. Braun and R. Herrmann, *Dalton Trans.*, 2016, **45**, 4716–4728.
98 A. K. Brisdon, I. R. Crossley, R. G. Pritchard and J. E. Warren, *Inorg. Chem.*, 2002, **41**, 4748–4755.
99 A. K. Brisdon, I. R. Crossley, J. A. Greenall, R. G. Pritchard and J. E. Warren, *J. Fluorine Chem.*, 2004, **125**, 1099–1103.
100 U. von Allwörden and G. V. Röschenthaler, *Chem.-Ztg.*, 1988, **112**, 69–76.
101 F. A. Akkerman, R. Kickbusch and D. Lentz, *Chem. – Asian J.*, 2008, **3**, 719–731.
102 H. Wessolowski, G.-V. Roschenthaler, R. Winter and G. L. Gard, *Phosphorus, Sulfur Silicon Relat. Elem.*, 1991, **60**, 201–208.
103 R. N. Haszeldine, D. W. Keen and A. E. Tipping, *J. Chem. Soc. C*, 1970, 414–421.
104 A. Bach, D. Lentz, P. Luger, M. Messerschmidt, C. Olesch and M. Patzschke, *Angew. Chem., Int. Ed.*, 2002, **41**, 296–299, (*Angew. Chem.*, 2002, **114**, 311–314).
105 D. Lentz, A. Bach, J. Buschmann, P. Luger and M. Messerschmidt, *Chem. – Eur. J.*, 2004, **10**, 5059–5066.
106 A. K. Brisdon, R. G. Pritchard and A. Thomas, *Organometallics*, 2012, **31**, 1341–1348.
107 B. M. Kraft, R. J. Lachicotte and W. D. Jones, *Organometallics*, 2002, **21**, 727–731.

108 B. M. Kraft, R. J. Lachicotte and W. D. Jones, *J. Am. Chem. Soc.*, 2000, **122**, 8559–8560.
109 T. Xiao-Jun and C. Qing-Yun, *Chem. Sci.*, 2012, **3**, 1694–1697.
110 J. Xiao, J. Wu, W. Zhao and S. Cao, *J. Fluorine Chem.*, 2013, **146**, 76–79.
111 T. Ichitsuka, T. Fujita, T. Arita and J. Ichikawa, *Angew. Chem., Int. Ed.*, 2014, **53**, 7564–7568, (*Angew. Chem.*, 2014, **162**, 7694–7698).
112 T. Ichitsuka, T. Fujita and J. Ichikawa, *ACS Catal.*, 2015, **5**, 5947–5950.
113 T. Fujita, T. Arita, T. Ichitsuka and J. Ichikawa, *Dalton Trans.*, 2015, **44**, 19460–19463.
114 S. Sabater, J. A. Mata and E. Peris, *Nat. Commun.*, 2013, **4**, 2553.
115 S. Yoshida, K. Shimomori, Y. Kim and T. Hosoya, *Angew. Chem., Int. Ed.*, 2016, **55**, 10406–10409, (*Angew. Chem.*, 2016, **128**, 10562–10565).
116 K. Fuchibe and T. Akiyama, *J. Am. Chem. Soc.*, 2006, **128**, 1434–1435.
117 (*a*) H. Dang, A. M. Whittaker and G. Lalic, *Chem. Sci.*, 2016, **7**, 505–509; (*b*) M. Tomoya, I. Yoshiteru and M. Masahiro, *Chem. Lett.*, 2008, **37**, 1006–1007.
118 T. Stahl, H. F. T. Klare and M. Oestreich, *ACS Catal.*, 2013, **3**, 1578–1587.
119 V. J. Scott, R. Çelenligil-Çetin and O. V. Ozerov, *J. Am. Chem. Soc.*, 2005, **127**, 2852–2853.
120 R. Panisch, M. Bolte and T. Müller, *J. Am. Chem. Soc.*, 2006, **128**, 9676–9682.
121 M. Klahn, C. Fischer, A. Spannenberg, U. Rosenthal and I. Krossing, *Tetrahedron Lett.*, 2007, **48**, 8900–8903.
122 C. Douvris and O. V. Ozerov, *Science*, 2008, **321**, 1188–1190.
123 R. N. Perutz, *Science*, 2008, **321**, 1168–1169.
124 W. Gu, M. R. Haneline, C. Douvris and O. V. Ozerov, *J. Am. Chem. Soc.*, 2009, **131**, 11203–11212.
125 H. F. T. Klare and M. Oestreich, *Dalton Trans.*, 2010, **39**, 9176–9184.
126 W. Gu and O. V. Ozerov, *Inorg. Chem.*, 2011, **50**, 2726–2728.
127 C. B. Caputo and D. W. Stephan, *Organometallics*, 2012, **31**, 27–30.
128 R. Azhakar, H. W. Roesky, H. Wolf and D. Stalke, *Chem. Commun.*, 2013, **49**, 1841–1843.
129 T. Stahl, H. F. T. Klare and M. Oestreich, *J. Am. Chem. Soc.*, 2013, **135**, 1248–1251.
130 M. Ahrens, G. Scholz, T. Braun and E. Kemnitz, *Angew. Chem., Int. Ed.*, 2013, **52**, 5328–5332, (*Angew. Chem.*, 2013, **125**, 5436–5440).
131 J. Zhu, M. Pérez, C. B. Caputo and D. W. Stephan, *Angew. Chem., Int. Ed.*, 2016, **55**, 1417–1421, (*Angew. Chem.*, 2016, **128**, 1439–1443).
132 B. Calvo, J. Wuttke, T. Braun and E. Kemnitz, *ChemCatChem*, 2016, **8**, 1945–1950.
133 M. Dryzhakov and J. Moran, *ACS Catal.*, 2016, 3670–3673.
134 J. Terao, M. Nakamura and N. Kambe, *Chem. Commun.*, 2009, 6011–6013.
135 T. Akiyama, K. Atobe, M. Shibata and K. Mori, *J. Fluorine Chem.*, 2013, **152**, 81–83.
136 P. H. M. Budzelaar, *gNMR, Version 4.1*, Adept Scientific plc, Letchworth, 2001.
137 R. Fuchs and H. Gilman, *J. Org. Chem.*, 1957, **22**, 1009–1011.
138 W. Wolfsberger, *J. Prakt. Chem./Chem.-Ztg.*, 1992, **334**, 453–464.
139 T. Schwier and V. Gevorgyan, *Org. Lett.*, 2005, **7**, 5191–5194.
140 V. G. Lakhtin, S. P. Knyazev, K. V. Pavlov, L. E. Gusel'nikov, E. N. Buravtseva, N. A. Kuyantseva, L. A. Parshkova, A. A. Mid'ko, V. G. Bykovchenko, A. V. Kisin and E. A. Chernyshev, *Russ. J. Gen. Chem.*, 2008, **78**, 898–902.
141 A. Jana, D. Ghoshal, H. W. Roesky, I. Objartel, G. Schwab and D. Stalke, *J. Am. Chem. Soc.*, 2009, **131**, 1288–1293.
142 Y. Ichinose, K. Nozaki, K. Wakamatsu, K. Oshima and K. Utimoto, *Tetrahedron Lett.*, 1987, **28**, 3709–3712.
143 Y. Ichinose, K. Nozaki, K. Wakamatsu, K. Oshima and K. Utimoto, *Tetrahedron Lett.*, 1987, **28**, 3709–3712.
144 S. Bernardoni, M. Lucarini, G. F. Pedulli, L. Valgimigli, V. Gevorgyan and C. Chatgilialoglu, *J. Org. Chem.*, 1997, **62**, 8009–8014.
145 W. Russell Bowman, S. L. Krintel and M. B. Schilling, *Org. Biomol. Chem.*, 2004, **2**, 585–592.
146 M. Zyder and T. Szymanska-Buzar, *J. Organomet. Chem.*, 2009, **694**, 2110–2113.
147 V. Y. Lee and A. Sekiguchi, in *Organometallic Compounds of Low-Coordinate Si, Ge, Sn and Pb*, John Wiley & Sons, Ltd, 2010, pp. 45–88.
148 Y. Ichinose, H. Oda, K. Oshima and K. Utimoto, *Bull. Chem. Soc. Jpn.*, 1987, **60**, 3468–3470.
149 F. Wada, S. Abe, N. Yonemaru, K. Kikukawa and T. Matsuda, *Bull. Chem. Soc. Jpn.*, 1991, **64**, 1701–1703.
150 E. Piers and R. Lemieux, *J. Chem. Soc., Perkin Trans. 1*, 1995, 3–5.
151 R. A. Widenhoefer, A. Vadehra and P. K. Cheruvu, *Organometallics*, 1999, **18**, 4614–4618.
152 T. Nakano, K. Ono, Y. Senda and T. Migita, *J. Organomet. Chem.*, 2001, **619**, 313–317.
153 B. Marciniec and H. Lawicka, *Appl. Organomet. Chem.*, 2008, **22**, 510–515.
154 T. Matsuda, S. Kadowaki, Y. Yamaguchi and M. Murakami, *Org. Lett.*, 2010, **12**, 1056–1058.
155 M. Itazaki, M. Kamitani and H. Nakazawa, *Chem. Commun.*, 2011, **47**, 7854–7856.
156 M. D. Greenhalgh and S. P. Thomas, *Chem. Commun.*, 2013, **49**, 11230–11232.
157 J. Pyziak, J. Walkowiak, M. Hoffmann and B. Marciniec, *J. Organomet. Chem.*, 2015, **794**, 96–103.
158 S. Schweizer, C. Tresse, P. Bisseret, J. Lalevee, G. Evano and N. Blanchard, *Org. Lett.*, 2015, **17**, 1794–1797.
159 S. Pelzer, B. Neumann, H. G. Stammler, N. Ignat'ev and B. Hoge, *Chem. – Eur. J.*, 2016, **22**, 3327–3332.
160 S. Pelzer, B. Neumann, H. G. Stammler, N. Ignat'ev and B. Hoge, *Chem. – Eur. J.*, 2016, **22**, 4758–4763.

161 B. Hoge, S. Pelzer and N. Ignat'ev (Merck Patent GmbH), WO2015/049034A1, 2014.
162 T. Yoshida, D. L. Thorn, T. Okano, S. Otsuka and J. A. Ibers, *J. Am. Chem. Soc.*, 1980, **102**, 6451–6457.
163 K. Mochida, T. Kugita and Y. Nakadaira, *Polyhedron*, 1990, **9**, 2263–2266.
164 S. P. Komanduri, A. C. Schrick, C. L. Feasley, C. P. Dufresne and C. S. Weinert, *Eur. J. Inorg. Chem.*, 2016, **2016**, 3196–3203.
165 G. M. Sheldrick and T. R. Schneider, *SHELXL: High-resolution refinement*, 1997.
166 G. M. Sheldrick, *SHELXL-2013, Program for Crystal Structure Refinement*, University of Göttingen, 2013.
167 G. M. Sheldrick, *SHELXS-2013, Program for Crystal Structure Solution*, University of Göttingen, 2013.
168 G. M. Sheldrick, *SADABS, Program for Empirical Absorption Correction*, University of Göttingen, 1996.
169 M. J. Frisch, G. W. Trucks, H. B. Schlegel, G. E. Scuseria, M. A. Robb, J. R. Cheeseman, G. Scalmani, V. Barone, B. Mennucci, G. A. Petersson, H. Nakatsuji, M. Caricato, X. Li, H. P. Hratchian, A. F. Izmaylov, J. Bloino, G. Zheng, J. L. Sonnenberg, M. Hada, M. Ehara, K. Toyota, R. Fukuda, J. Hasegawa, M. Ishida, T. Nakajima, Y. Honda, O. Kitao, H. Nakai, T. Vreven, J. A. Montgomery Jr., J. E. Peralta, F. Ogliaro, M. Bearpark, J. J. Heyd, E. Brothers, K. N. Kudin, V. N. Staroverov, T. Keith, R. Kobayashi, J. Normand, K. Raghavachari, A. Rendell, J. C. Burant, S. S. Iyengar, J. Tomasi, M. Cossi, N. Rega, J. M. Millam, M. Klene, J. E. Knox, J. B. Cross, V. Bakken, C. Adamo, J. Jaramillo, R. Gomperts, R. E. Stratmann, O. Yazyev, A. J. Austin, R. Cammi, C. Pomelli, J. W. Ochterski, R. L. Martin, K. Morokuma, V. G. Zakrzewski, G. A. Voth, P. Salvador, J. J. Dannenberg, S. Dapprich, A. D. Daniels, O. Farkas, J. B. Foresman, J. V. Ortiz, J. Cioslowski and D. J. Fox, *Gaussian 09, Revision D.01*, Gaussian, Inc., Wallingford CT, 2013.
170 K. A. Peterson, D. Figgen, M. Dolg and H. Stoll, *J. Chem. Phys.*, 2007, **126**, 124101.